

Shearing of frictional sphere packings

Jean-François Métayer, * Donald J. Suntrup III, †
Charles Radin, ‡ Harry L. Swinney † Matthias Schröter *

January 21, 2010

Submitted to the themed issue on granular and jammed materials.

Abstract

We measure shear stress in packings of glass spheres by pulling a thin metal plate vertically through a bed of volume fractions ϕ , which is set (before the plate is pulled) to be in the range 0.575 to 0.628. The yield stress increases exponentially with ϕ with a change in slope at $\phi \approx 0.594$. An analysis of the shear stress fluctuations provides a measure of the shear modulus divided by shear zone width; this measure also exhibits distinct regimes above and below $\phi \approx 0.594$. The yield stress and the rescaled shear modulus are velocity independent over 4 decades.

1 Introduction

The jamming paradigm proposed by Liu and Nagel¹ in 1998 has stimulated an extensive effort to develop a unified picture of jamming/unjamming in particulate soft-matter systems such as colloids, foams and emulsions. However, most of this numerical²⁻⁶ and experimental⁷ work has been done for frictionless particles, while the interaction between granular particles involves friction and, consequently, departures from the jamming paradigm. This is most apparent in the range of volume fractions ϕ in which

*Max Planck Institute for Dynamics and Self-Organization

†Center for Nonlinear Dynamics and Department of Physics, University of Texas at Austin

‡Department of Mathematics, University of Texas at Austin

mechanically stable packings exist. For frictionless spheres the lower limit is $\phi \approx 0.64$, while packings of frictional spheres are stable down to $\phi \approx 0.55$, the so-called random loose packing^{8,9} limit. Numerical studies of jamming in frictional systems¹⁰⁻¹⁵ have been helpful but not definitive, and there is a need for experimental clarification.

In probing experimentally the mechanical properties of granular matter it is advantageous¹⁶ to disentangle the contributions from compression and shear. This is not possible in penetration tests¹⁷⁻²¹ where the tip of a rod advancing in a granular sample will both shear and compress the sample. Coming from the fluid side, one can also try to determine the onset of jamming from rheological measurements of granular suspensions.^{22,23} However, in the absence of perfect density matching between particles and liquid, shear bands make the results hard to interpret.²² Contributions of shear and compression could be separated with a triaxial shear tester,²⁴ which would however complicate the control of the probed volume fraction. Precise data have been obtained for 2-dimensional collections of photoelastic discs;^{25,26} an advantage of the restriction to two dimensions is that one can additionally obtain local information.²⁷

In this paper we present experimental results showing how 3-dimensional packings with frictional particles yield when sheared. After describing our experimental setup we will present results on the yield stress and rescaled shear modulus and the results will be discussed in the context of jamming paradigm and dilatancy onset.

2 Experiment

Our experimental set-up [Fig. 1] consists of a vertical glass tube (diameter 38.7 mm, height 300 mm) filled with water and soda-lime glass beads (diameter $d = 200 \pm 10 \mu\text{m}$). The packing fraction ϕ is controlled using flow pulses²¹ created by a computer-controlled gear pump. The granular bed is fluidized during flow pulses of 1 min duration, followed by a 2 min settling time during which the bed completely sediments. The packing fraction after sedimentation depends on the flow rate during the fluidization phase: loose packings are obtained using a small number of pulses of flow rates on the order of 50 ml/min, while larger packing fractions are obtained by fluidizing the

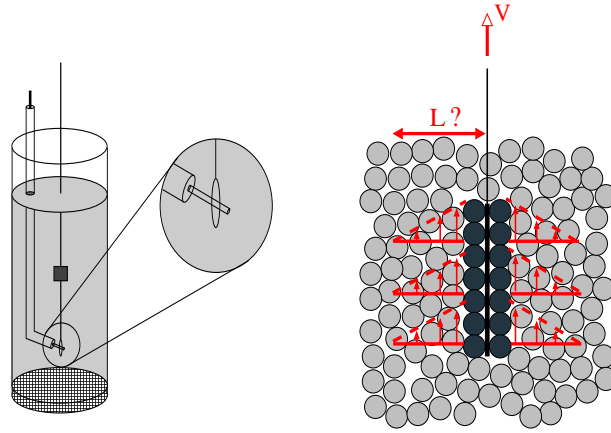


Fig. 1 Left: a sketch of the experimental setup. The enlargement shows how the plate and nylon thread are held in place during fluidization by a rod, which is then withdrawn during the measurements. Right: cartoon of the sheared zone with the a priori unknown size L of the sheared region.

granular bed repeatedly with pulses of decreasing flow rates.

To measure the shear force needed to initiate a displacement in the granular bed, a thin metallic plate (12.8 mm high \times 9.8 mm wide \times 0.1 mm thick) is pulled vertically through the bed. Both sides of the plate are covered with glass beads (glued there with 3M Bonding film 583); the resulting total thickness of the plate is 0.6 mm. The plate is immersed in the bed before fluidization and is connected to a load cell (Honeywell Sensotec Model 31, range 250 g) by a nylon thread (diameter 150 μ m, length 275 mm, elastic constant $7 \times 10^{-4} \text{N}^{-1}$). To keep the plate in place during the fluidization, a nylon thread is attached to the plate bottom and the other end of the thread is attached to a plastic rod [cf. Fig. 1]. After the sedimentation following the fluidization pulses, the plastic rod is withdrawn through a metallic cylinder to minimize disturbances to the granular bed. Then the plate is free to move.

During a measurement, a translation stage driven by a DC-Servo motor pulls the plate upwards over a distance of 2 mm at a constant velocity of 0.15 mm/min (except for a set of measurements made to determine the velocity dependence). Before the measurement the upper edge of the plate is 160 ± 5 mm below the sand surface. The shear force is measured with the load cell connected to a bridge amplifier (Omega DMD-465WB); its output voltage is digitized with a 16 bit data acquisition card (NI

PCI-6036E) at a frequency of 100 Hz. This corresponds to one data point every $1 * 10^{-4}$ grain diameters. The noise level of this setup corresponds to about 1 mN, as determined from a measurement done in an empty tube.

3 Results

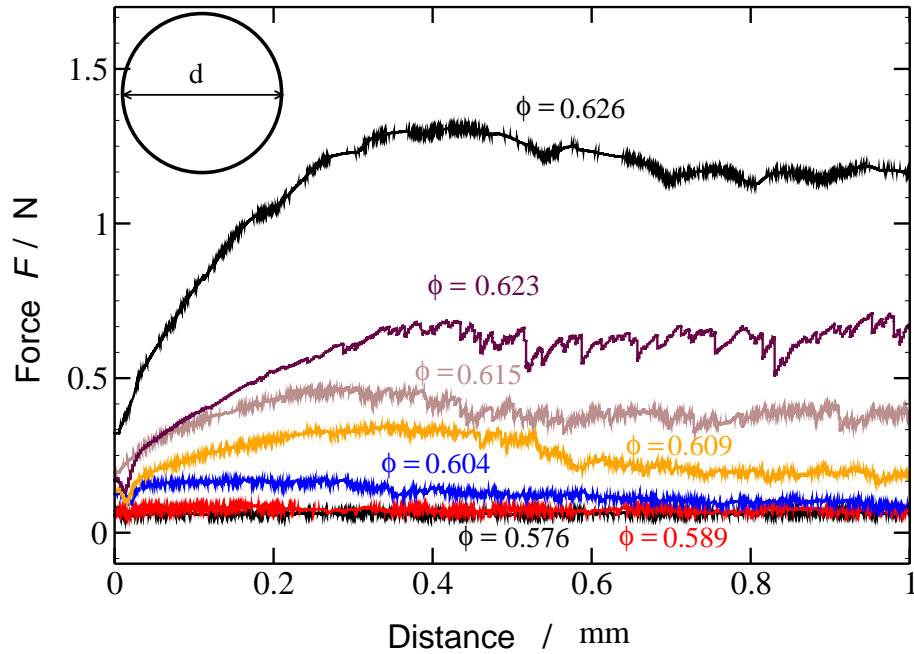


Fig. 2 Force needed to pull the plate up at different packing fractions.

Typical force measurements, as a function of the displacement of the plate, are presented in Fig. 2. For low packing fraction (below 0.59) the force is constant for the whole displacement. For higher ϕ , the force reaches a maximum value in the first 0.5mm before it begins to decrease again. We consider this maximum to be the yield stress, the force needed to initiate a reorganization of the structure of the bed. This yield force is measured as the average over a length of approximately two grain diameters centered on the position of the maximum. The dependence of this yield force on packing fraction is shown in the inset of Fig. 3 (open circles).

The forces we measure result not only from the shear at the sidewalls of the plate;

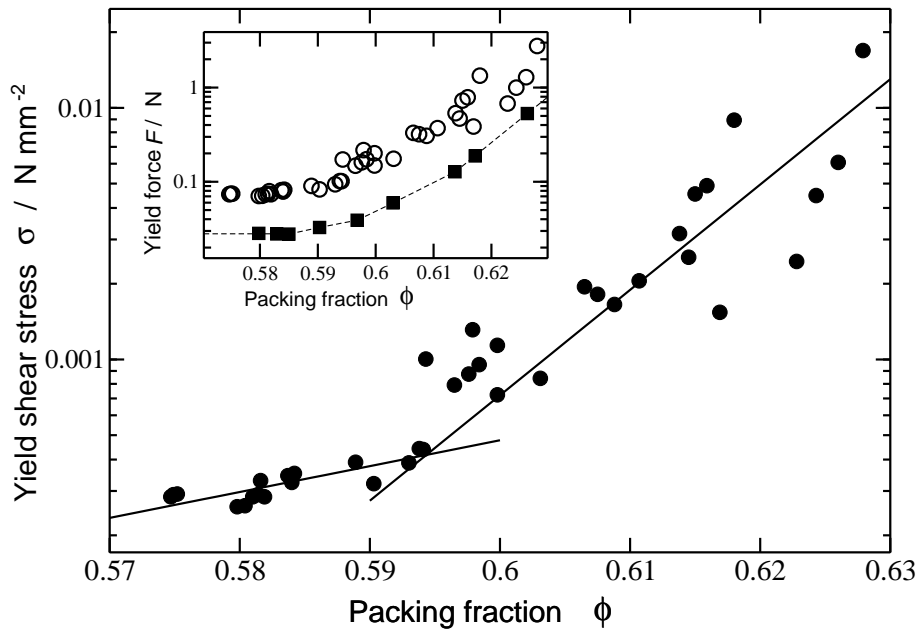


Fig. 3 Yield shear stress as a function of the volume fraction. The inset shows the force needed to pull the plate (open circles) and to pull a horizontal rod of the same dimensions as the upper edge of the plate (filled squares). The pure shear yield component shown in the main plot was obtained from the data in the inset by subtracting the dashed line from the data given by the open circles. (The datum at the highest volume fraction was taken with a Model 31 load cell with the range 1 kg.) The solid lines are exponential fits for packing fractions below and above 0.5942; the lines intersect at $\phi = 0.5943$.

there is also a compression component due to the upward motion of the top edge of the plate. To determine the value of this compression component we made measurements using a horizontal cylindrical rod which has the same length as the plate width (9.8mm) and a diameter the same as the thickness of the plate (0.6mm). Results for different packing fractions are shown in the inset of Fig. 3 (filled square). The yield shear stress is then obtained by subtracting the compression component (which is obtained by fitting each couple of successive points by an exponential function) from measurements made with the plate and by dividing the results by its area (125.4mm^2) [Fig. 3]. Though the data are noisy, there is a clear change in slope at $\phi \approx 0.594$.

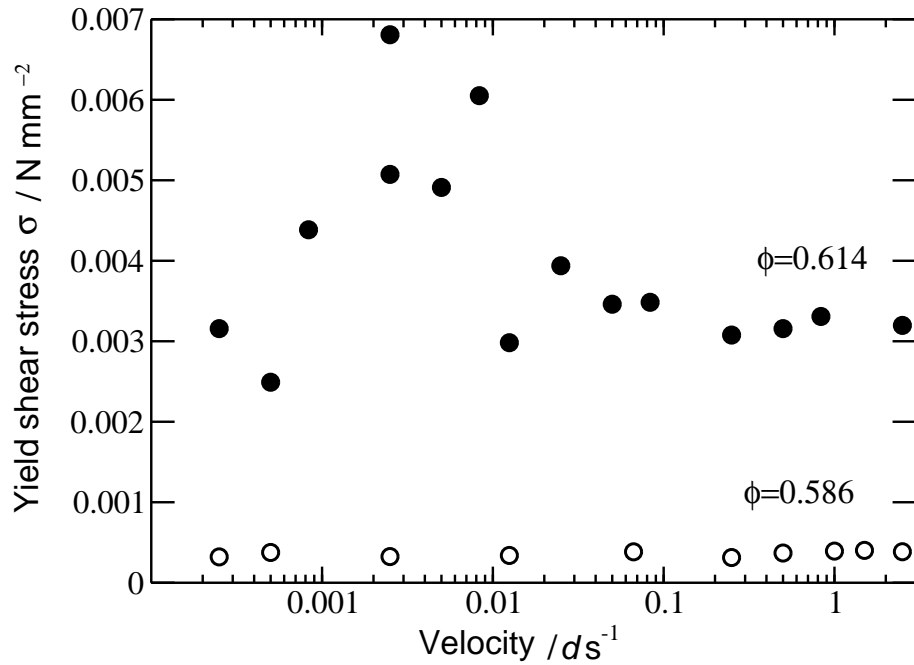


Fig. 4 The yield stress is velocity independent. All other measurement presented in this paper were done at a velocity of 0.0125 grain diameters per second.

Fig. 4 shows that the measured yield stress is independent of the velocity of the plate, both above and below $\phi = 0.594$. The larger fluctuations at lower velocities and higher packing fractions are an unexpected result.

The fluctuations in the force measurements shown in Fig. 2 contain information concerning the shear modulus of the granular medium as a function of the packing

fraction. Fig. 5 shows on an expanded scale a force measurement as a function of position for $\phi = 0.623$. Smooth “elastic” increases of the force are followed by rapid plastic decreases, very similar to stick-slip motion. The frequency of the jumps is found to be independent of the velocity of the plate. An analysis of the fluctuations, inspired by work of Cantat and Pitois,²⁸ yields the shear modulus: $G = \frac{\Delta F}{\Delta x} * \frac{L}{A}$. The ratio $\Delta F/\Delta x$ is the slope of the elastic increases we observe, as illustrated in Fig. 5, L is the width of the sheared zone around the plate [Fig. 1] and A the area of the plate. To calculate the shear modulus we need to know the lengthscale L , but its value has not been determined. Therefore, we compute the shear modulus per length, $g^* = \frac{G}{L}$.

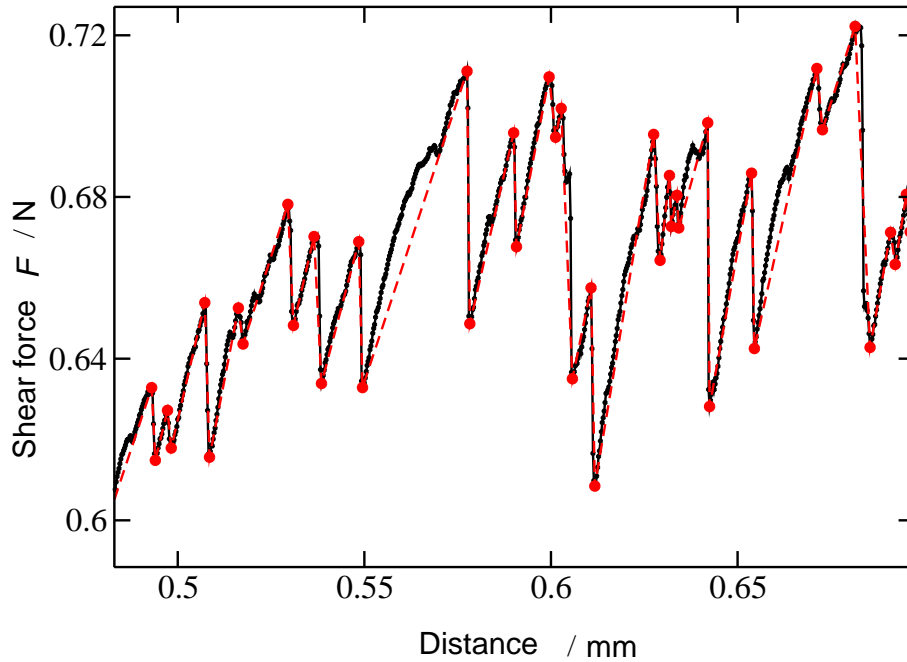


Fig. 5 Identification of stick-slip events in the yielding regime. The solid black line is the raw data, and the red dots are the minima and maxima. Consecutive extremas are separated by at least $5mN$, which corresponds to 5 times the noise level.

Knowing the value and the position of each extremum, we compute the slope, the amplitude, and the duration of elastic loading and the plastic relaxation. The displacement during a plastic jump downward (typically 5×10^{-3} grain diameters) is well resolved in our measurements, where measurements are made with a typical mesh of 1×10^{-4} grain diameters.

The probability distributions for the shear modulus per unit length, g^* , for packing fractions below the transition at $\phi = 0.594$ are different from the distributions above the transition, but each is well-defined (cf. Fig. 6). Further, as Fig. 7 illustrates, g^* behaves differently below and above $\phi = 0.594$, which is the same packing fraction value obtained for the transition observed in the shear stress. The shear modulus per unit length, g^* , is found to be velocity-independent for a wide range of forcings, just as we found for the shear stress.

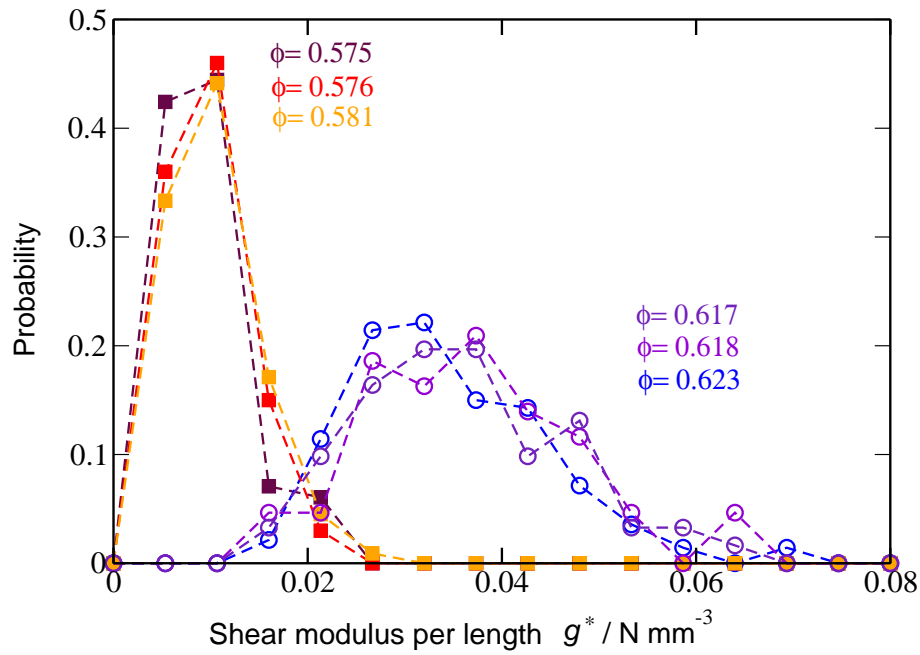


Fig. 6 The probability distribution functions for the shear modulus per unit length g^* for packing fractions ϕ above and below the transition value, $\phi = 0.594$.

The values of g^* in Fig. 7 obtained for the two highest packing fraction values are well below the line given by the nearby data. To determine the origin of this unexpected behaviour we compute the amplitude of elastic loads [Fig. 8 top] and their length, as a function of packing fraction [Fig. 8 bottom]. As can be seen, the low values of g^* for packing fractions higher than 0.623 arise not because of a decrease of the elastic loads amplitude but because of an increase of their length.

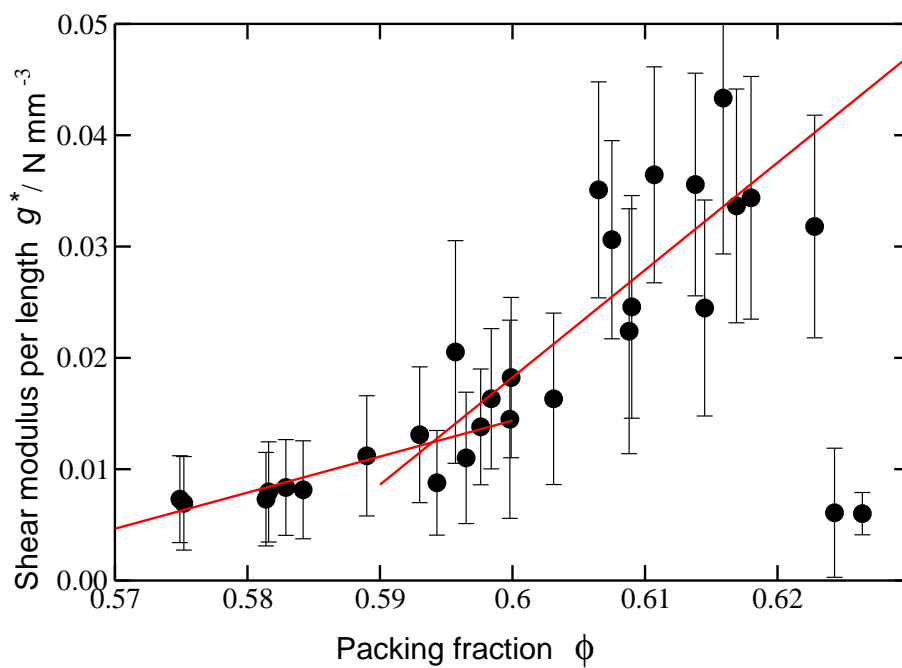


Fig. 7 The shear modulus per unit length exhibits a transition at $\phi = 0.594$, as given by the intersection of the red lines which were fit to the data below and above 0.5937 (not included in fit: the g^* values obtained for the two highest values of ϕ). The error bars correspond to the standard deviation of g^* distributions ([Fig. 6]).

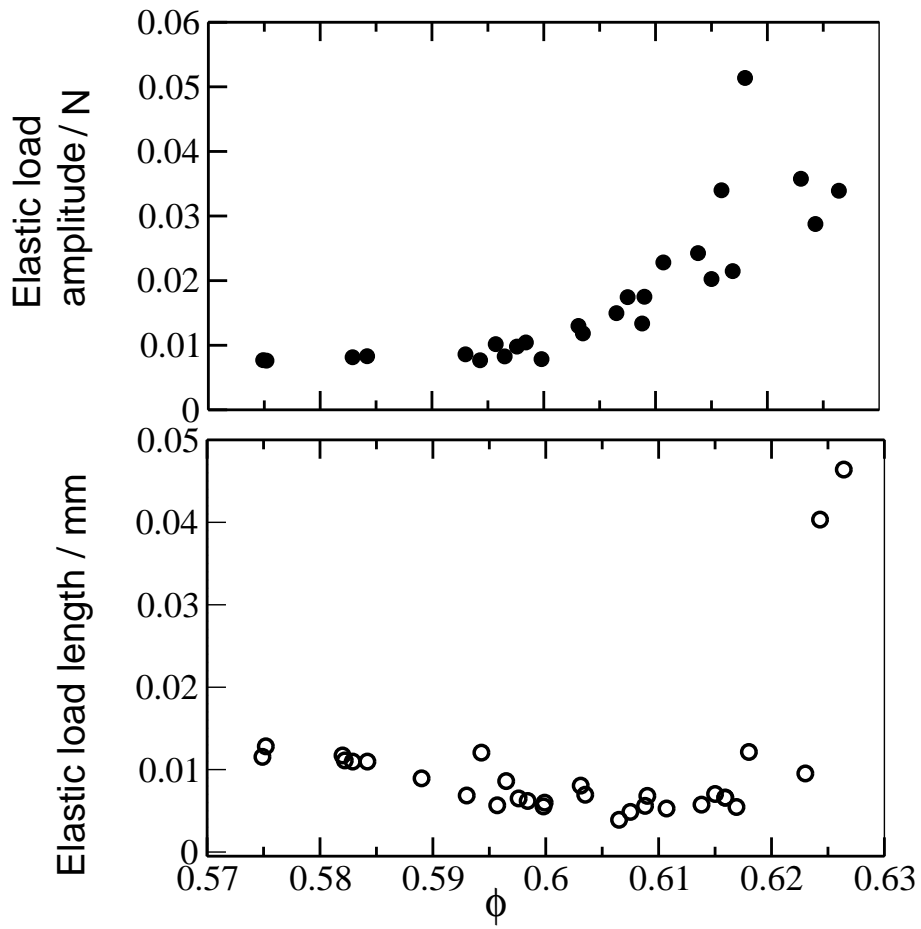


Fig. 8 Top: average force increase during elastic loading, bottom: average length of the elastic events.

4 Discussion

Our results are consistent with the previously observed transition at $\phi \approx 0.595$.²¹ Both the transition and dilatancy onset concern the response of the system to shear, the former in terms of a sharp change in yield stress, and the latter in terms of the sign of the change of volume fraction due to shear. The interpretation of the two as the same phenomenon is consistent with previous results.^{21,29,30}

In comparing our results with the jamming paradigm we first note a conceptual ambiguity: what is the equivalent in granular systems of point J in the frictionless jamming phase diagram? Possible candidates are the random loose packing density $\phi = 0.55$, the transition value we report here, $\phi = 0.594$, and the random close packing density $\phi = 0.64$.

For simulations of nonfrictional, soft particles the value $\phi = 0.64$ corresponds to two phenomena: a) the lower limit in which the system supports a positive yield stress and b) the only possible density of amorphous packings of undeformed, pressure free spheres. Denser packings can only be built from compressed spheres and therefore need to have a finite pressure. This property is independent of friction and therefore also applicable in our granular system. A recent 2D experiment²⁷ has suggested that point J might indeed describe frictional systems near random close packing.

However, with friction there exists, for any positive pressure, mechanically stable states at a continuum of packing fractions below $\phi = 0.64$. The lowest volume fraction then depends on pressure and friction.^{9,13} Its zero pressure limit is the random loose packing limit, and in recent work it has been repeatedly taken as point J.^{9,11,13}

Finally, the onset of dilatancy at $\phi \approx 0.594$ might also bear some resemblance to point J. In a closed volume ensemble any shear at higher densities would require strong deformation of the particles.

One possible way to resolve the ambiguity in the identification of the J point with the observed transitions would be to use an ensemble-based theory, such as that of Edwards and coworkers,³¹ to explain the observed behavior of granular matter throughout the full range $0.55 < \phi < 0.74$. From such a theory one could compute the response of

the material to shear, to elucidate the observed behavior at $\phi = 0.594$ and 0.64 . This has not yet been done.

We would also like to note that the yield stress presented in Fig. 3 corresponds to the jammed-unjammed transition in the base plane of the classical jamming phase diagram,^{1,3} at least for a given pressure. And once the length of the shear zone has been determined independently, the volume fraction dependence of g^* in Fig. 7 can be compared to the power laws^{2,3} found for the shear modulus in simulations of nonfrictional particles.

The velocity independence of both the yield shear stress and the shear modulus per length contrast with the previously observed logarithmic velocity dependence in sheared 2-dimensional photoelastic discs.^{25,26} This might be either related to the difference in dimensionality or to the different values of the Young's moduli of the materials used: 70 GPa/m^2 for the glass beads and 4 MPa/m^2 for the photoelastic discs.

An interesting question open question is the role of pressure in these results. Previous measurements have shown that, even at a constant depth in the sample as in our measurements, the pressure depends on volume fraction and preparation.³² Therefore, future work should include independent measurements of pressure.

In this paper we focused on unjamming properties under shear of 3-dimensional packings of frictional spheres. We show that both yield shear stress and shear modulus per length present a transition at packing fraction $\phi \approx 0.594$. Additionally the shear stress is shown to be velocity independent in a range of four decades. This velocity independence was found below and above $\phi \approx 0.594$. As mentioned, this particular value of ϕ could be the dilatancy onset.

Acknowledgments We would like to thank Udo Krafft for experimental support. This research was supported in part by Welch Foundation Grant F-0805 and NSF Grant DMS-0700120.

References

- [1] A. J. Liu and S. R. Nagel, *Nature*, 1998, **396**, 21 – 22.

- [2] H. A. Makse, N. Gland, D. L. Johnson and L. M. Schwartz, *Phys. Rev. Lett.*, 1999, **83**, 5070.
- [3] C. S. O'Hern, L. E. Silbert, A. J. Liu and S. R. Nagel, *Phys. Rev. E*, 2003, **68**, 011306.
- [4] P. Olsson and S. Teitel, *Phys. Rev. Lett.*, 2007, **99**, 178001.
- [5] C. Heussinger and J. Barrat, *Phys. Rev. Lett.*, 2009, **102**, 218303.
- [6] M. Pica Ciamarra and A. Coniglio, *Phys. Rev. Lett.*, 2009, **103**, 235701.
- [7] G. Katgert, *Ph.D. thesis*, Universiteit Leiden, 2008.
- [8] M. Pica Ciamarra and A. Coniglio, *Phys. Rev. Lett.*, 2008, **101**, 128001.
- [9] M. Jerkins, M. Schröter, H. L. Swinney, T. J. Senden, M. Saadatfar and T. Aste, *Phys. Rev. Lett.*, 2008, **101**, 018301.
- [10] L. E. Silbert, D. Ertaş, G. S. Grest, T. C. Halsey and D. Levine, *Phys. Rev. E*, 2002, **65**, 031304.
- [11] H. P. Zhang and H. A. Makse, *Phys. Rev. E*, 2005, **72**, 011301.
- [12] E. Somfai, M. van Hecke, W. G. Ellenbroek, K. Shundyak and W. van Saarloos, *Phys. Rev. E*, 2007, **75**, 020301.
- [13] K. Shundyak, M. van Hecke and W. van Saarloos, *Phys. Rev. E*, 2007, **75**, 010301.
- [14] V. Magnanimo, L. L. Ragoni, J. T. Jenkins, P. Wang and H. A. Makse, *Europhys. Lett.*, 2008, **81**, 34006.
- [15] S. Henkes, K. Shundyak, W. van Saarloos and M. van Hecke, arXiv:0911.5134.
- [16] W. G. Ellenbroek, Z. Zeravcic, W. van Saarloos and M. van Hecke, *Euro. Phys. Lett.*, 2009, **87**, 34004.
- [17] M. B. Stone, D. P. Bernstein, R. Barry, M. D. Pelc, Y. K. Tsui and P. Schiffer, *Nature*, 2004, **427**, 503–504.

- [18] M. B. Stone, R. Barry, D. P. Bernstein, M. D. Pelc, Y. K. Tsui and P. Schiffer, *Phys. Rev. E*, 2004, **70**, 041301.
- [19] G. Hill, S. Yeung and S. A. Koehler, *Europhys. Lett.*, 2005, **72**, 137–143.
- [20] M. Toiya, J. Hettinga and W. Losert, *Granular Matter*, 2007, **9**, 323 – 329.
- [21] M. Schröter, S. Nägle, C. Radin and H. L. Swinney, *Europhys. Lett.*, 2007, **78**, 44004.
- [22] A. Fall, F. Bertrand, G. Ovarlez and D. Bonn, *Phys. Rev. Lett.*, 2009, **103**, 178301.
- [23] E. Brown and H. M. Jaeger, *Phys. Rev. Lett.*, 2009, **103**, 086001.
- [24] P. Evesque, D. Fargeix, P. Habib, M. P. Luong and P. Porion, *Phys. Rev. E*, 1993, **47**, 2326–2332.
- [25] R. R. Hartley and R. P. Behringer, *Nature*, 2003, **421**, 928.
- [26] R. P. Behringer, D. Bi, B. Chakraborty, S. Henkes and R. R. Hartley, *Phys. Rev. Lett.*, 2008, **101**, 268301.
- [27] T. S. Majmudar, M. Sperl, S. Luding and R. P. Behringer, *Phys. Rev. Lett.*, 2007, **98**, 058001.
- [28] I. Cantat and O. Pitois, *Physics of Fluids*, 2006, **18**, 083302.
- [29] A. J. Kabla and T. J. Senden, *Phys. Rev. Lett.*, 2009, **102**, 228301.
- [30] N. Gravish, P. Umbanhowar and D. I. Goldman, *Bulletin of the American Physical Society*, 2009, **54**, 94, BU8.
- [31] S. F. Edwards and R. B. S. Oakeshott, *Physica A*, 1989, **157**, 1080–1090.
- [32] L. Vanel and E. Clément, *Eur. Phys. J. B*, 1999, **11**, 525–533.